Extraction of unpolarised TMDs from experimental data

Valerio Bertone
IRFU, CEA, DPhN, Université Paris-Saclay

March 10, 2021, Assemblée Générale du QCD

This project has received funding from the European Union's Horizon 2020 research and innovation programme under grant agreement № 824093

TMD factorisation (for DY)

- At **small values of q_T**, TMD factorisation applies:

$$\left(\frac{d\sigma}{dq_T}\right)_{\text{res.}} \stackrel{\text{TMD}}{=} \sigma_0 H(Q) \int d^2\mathbf{b}_T e^{i\mathbf{b}_T\cdot\mathbf{q}_T} F_1(x_1,\mathbf{b}_T,Q,Q^2) F_2(x_2,\mathbf{b}_T,Q,Q^2)$$

- The single TMD distributions are given by:

$$F_{f/P}(x,\mathbf{b}_T;\mu,\zeta) = \sum_j C_{f/j}(x,b_T;\mu_b,\zeta_F)\otimes f_{j/P}(x,\mu_b) \qquad : A$$

$$\times \exp\left\{K(b_T;\mu_b)\ln\frac{\sqrt{\zeta_F}}{\mu_b} + \int_{\mu_b}^{\mu}\frac{d\mu'}{\mu'}\left[\gamma_F - \gamma_K \ln\frac{\sqrt{\zeta_F}}{\mu'}\right]\right\} \qquad : B$$

TMD factorisation (for DY)

- At **small values of q_T**, TMD factorisation applies:

$$\left(\frac{d\sigma}{dq_T}\right)_{\text{res.}} \stackrel{\text{TMD}}{=} \sigma_0 H(Q) \int d^2\mathbf{b}_T e^{i\mathbf{b}_T\cdot\mathbf{q}_T} F_1(x_1, \mathbf{b}_T, Q, Q^2) F_2(x_2, \mathbf{b}_T, Q, Q^2)$$

- The single TMD distributions are given by:

$$F_{f/P}(x, \mathbf{b}_T; \mu, \zeta) = \boxed{\sum_j C_{f/j}(x, b_T; \mu_b, \zeta_F) \otimes f_{j/P}(x, \mu_b)} \quad : A$$

$$\times \boxed{\exp\left\{K(b_T; \mu_b) \ln \frac{\sqrt{\zeta_F}}{\mu_b} + \int_{\mu_b}^{\mu} \frac{d\mu'}{\mu'}\left[\gamma_F - \gamma_K \ln \frac{\sqrt{\zeta_F}}{\mu'}\right]\right\}} \quad : B$$

- matching onto the collinear PDFs at $b_T \ll 1/\Lambda_{QCD}$,
- factorises as *transverse* (perturbative) and *longitudinal* (*i.e.* collinear, non-perturbative).

- CS and RGE evolution,
- evolution to large b_T,
- perturbative.

TMD factorisation (for DY)

- At **small values of q_T**, TMD factorisation applies:

$$\left(\frac{d\sigma}{dq_T}\right)_{\text{res.}} \overset{\text{TMD}}{=} \sigma_0 H(Q) \int d^2\mathbf{b}_T e^{i\mathbf{b}_T\cdot\mathbf{q}_T} F_1(x_1,\mathbf{b}_T,Q,Q^2) F_2(x_2,\mathbf{b}_T,Q,Q^2)$$

- The single TMD distributions are given by:

$$F_{f/P}(x,\mathbf{b}_T;\mu,\zeta) = \sum_j C_{f/j}(x,b_*;\mu_b,\zeta_F)\otimes f_{j/P}(x,\mu_b) \qquad \left(\mu_b = 2e^{-\gamma_E}/b_*\right) : A$$

$$\times \exp\left\{K(b_*;\mu_b)\ln\frac{\sqrt{\zeta_F}}{\mu_b} + \int_{\mu_b}^{\mu}\frac{d\mu'}{\mu'}\left[\gamma_F - \gamma_K \ln\frac{\sqrt{\zeta_F}}{\mu'}\right]\right\} \qquad : B$$

$$\times \exp\left\{g_{j/P}(x,b_T) + g_K(b_T)\ln\frac{\sqrt{\zeta_F}}{\sqrt{\zeta_{F,0}}}\right\} \qquad : C$$

- Introduce the b_* prescription to avoid the Landau pole,
- introduce f_{NP} to account for the introduction of the b_* prescription,
- f_{NP} "parametrises" the non-perturbative transverse modes,
- **fit** f_{NP} to data.

Higher-order corrections

- Measurements of q_T distributions have reached the **sub-percent level** uncs.:

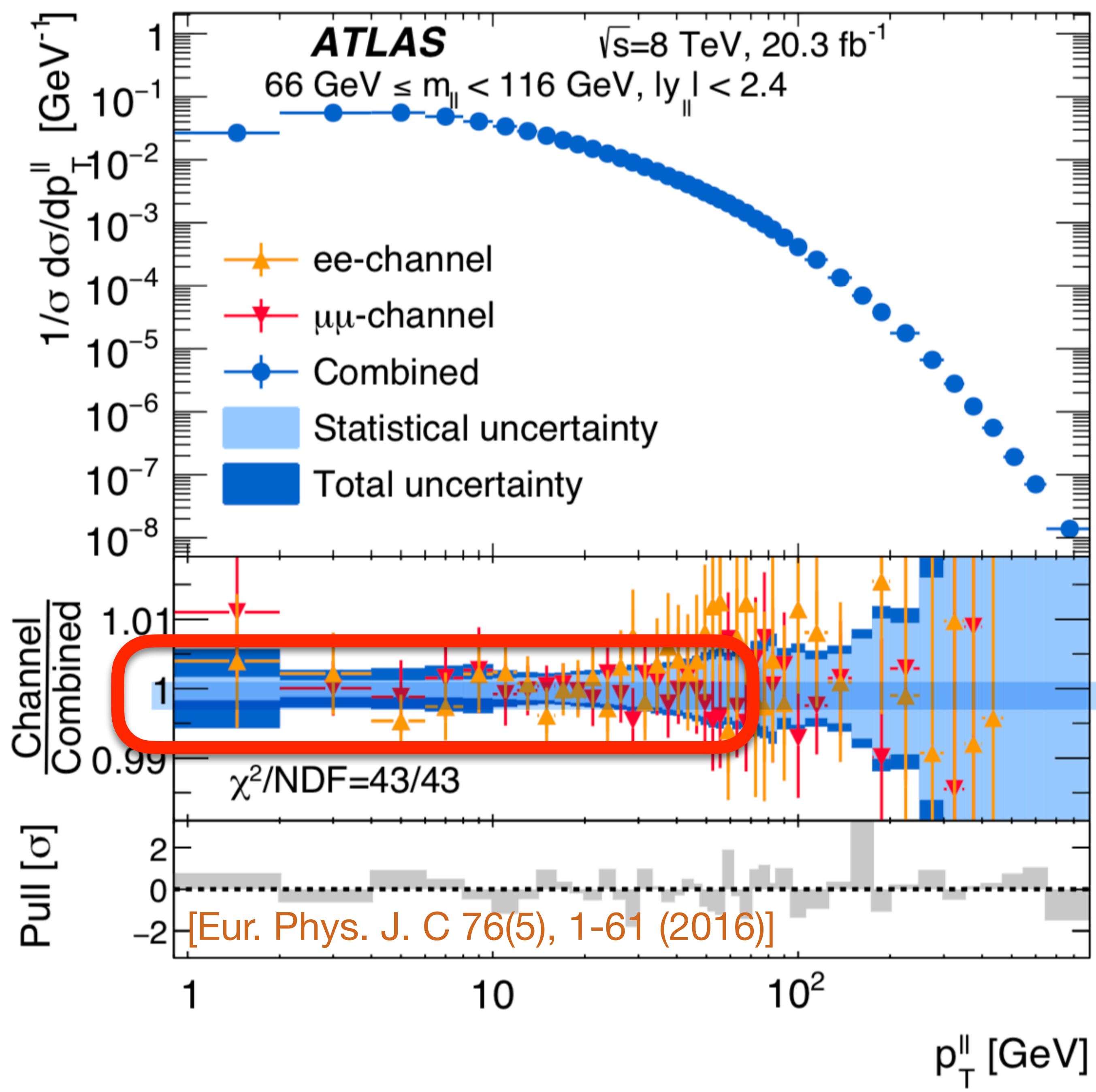

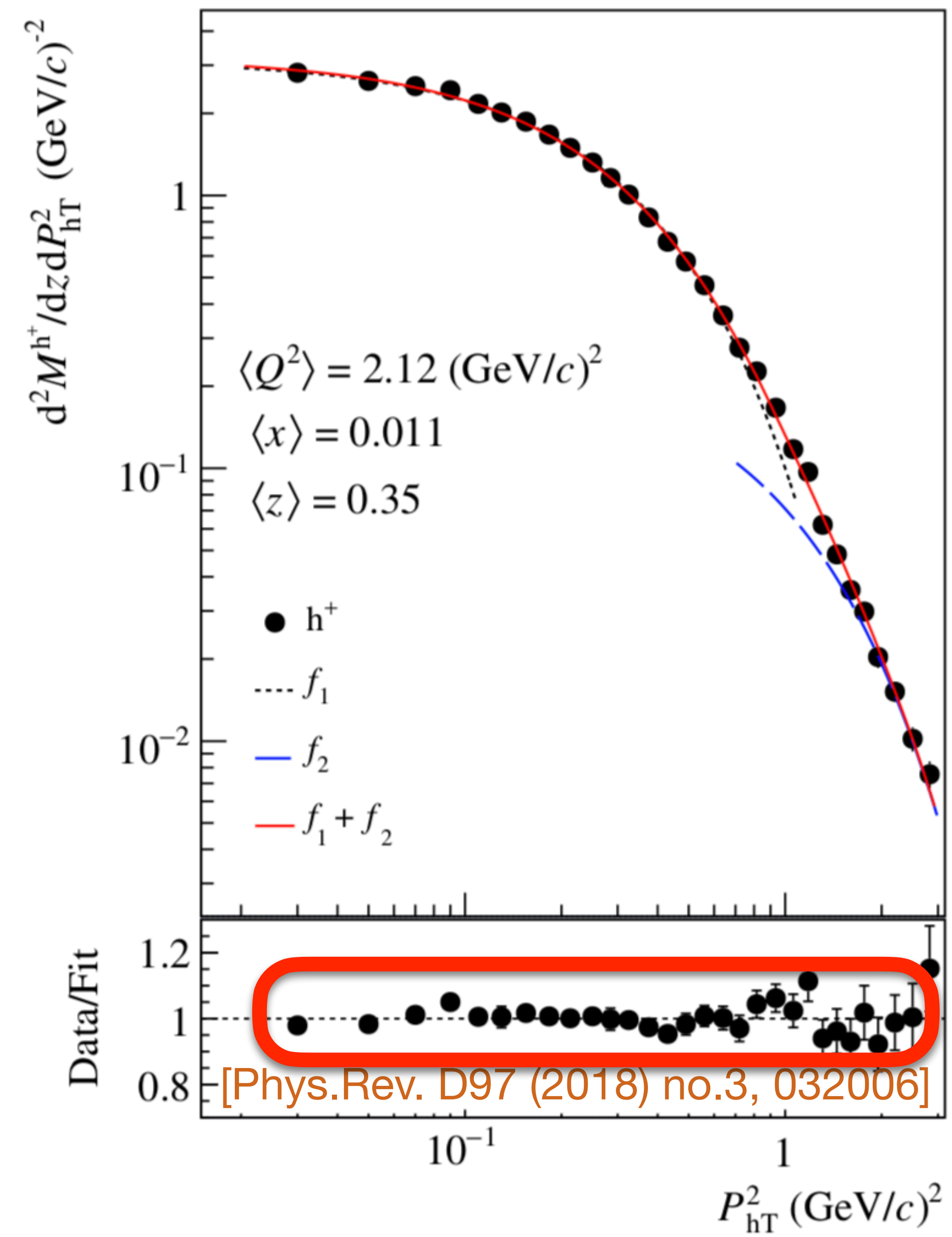

- **State-of-the-art** calculations are thus necessary to describe this data:
  - **higher-order** corrections (and possibly **matching** between **TMD** and **collinear**).

Higher-order corrections

- State-of-the-art accuracy in the TMD region required:

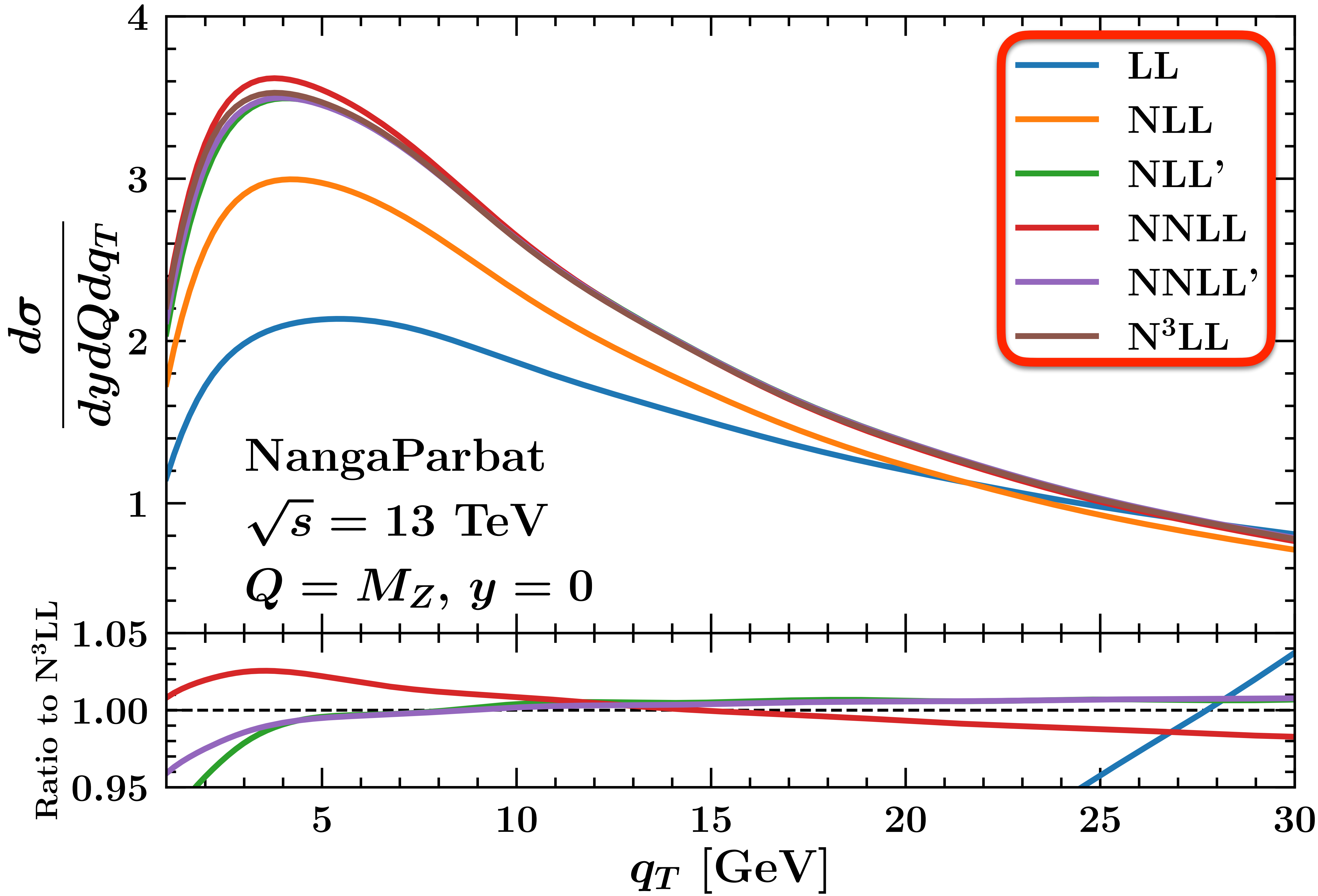

Pavia 2019 (PV19): the settings

[Bacchetta *et al.*, *JHEP* 07 (2020) 117, arXiv:1912.07550]

- Functional form of the non-perturbative function:

$$f_{\rm NP}(x, b_T, \zeta) = \left[\frac{1-\lambda}{1+g_1(x)\frac{b_T^2}{4}} + \lambda \exp\left(-g_{1B}(x)\frac{b_T^2}{4}\right)\right] \exp\left[-\left(g_2 + g_{2B} b_T^2\right) \ln\left(\frac{\zeta}{Q_0^2}\right)\frac{b_T^2}{4}\right]$$

$$g_1(x) = \frac{N_1}{x\sigma} \exp\left[-\frac{1}{2\sigma^2}\ln^2\left(\frac{x}{\alpha}\right)\right] \quad \text{and} \quad g_{1B}(x) = \frac{N_{1B}}{x\sigma_B} \exp\left[-\frac{1}{2\sigma_B^2}\ln^2\left(\frac{x}{\alpha_B}\right)\right]$$

  - a total of 9 free parameters.
- Complete treatment of the experimental uncertainties:
  - **correlated** systematics (additive and multiplicative) properly treated,
  - uncertainties deriving from **collinear PDFs** also included.
- Fits using all the available perturbative orders: **from NLL to N^{3}LL**.
- **Full integration** over q_T, Q and y when required:
  - no narrow-width nor "middle-point" approximations.
- No *ad hoc* **normalisation**:
  - fit both shape and normalisation.
- **Monte Carlo** method for the experimental error propagation.

PV19 fit: Drell-Yan data

Fixed target

RHIC

Tevatron

LHC

Experiment	N_{dat}	Observable	$\sqrt{s}$ [GeV]	Q [GeV]	y or x_F	Lepton cuts	Ref.
E605	50	$Ed^3\sigma/d^3q$	38.8	7 - 18	$x_F = 0.1$	-	[79]
E288 200 GeV	30	$Ed^3\sigma/d^3q$	19.4	4 - 9	$y = 0.40$	-	[80]
E288 300 GeV	39	$Ed^3\sigma/d^3q$	23.8	4 - 12	$y = 0.21$	-	[80]
E288 400 GeV	61	$Ed^3\sigma/d^3q$	27.4	5 - 14	$y = 0.03$	-	[80]
STAR 510	7	$d\sigma/dq_T$	510	73 - 114	$\|y\| < 1$	$p_{T\ell} > 25$ GeV $\|\eta_\ell\| < 1$	-
CDF Run I	25	$d\sigma/dq_T$	1800	66 - 116	Inclusive	-	[81]
CDF Run II	26	$d\sigma/dq_T$	1960	66 - 116	Inclusive	-	[82]
D0 Run I	12	$d\sigma/dq_T$	1800	75 - 105	Inclusive	-	[83]
D0 Run II	5	$(1/\sigma)d\sigma/dq_T$	1960	70 - 110	Inclusive	-	[84]
D0 Run II (μ)	3	$(1/\sigma)d\sigma/dq_T$	1960	65 - 115	$\|y\| < 1.7$	$p_{T\ell} > 15$ GeV $\|\eta_\ell\| < 1.7$	[85]
LHCb 7 TeV	7	$d\sigma/dq_T$	7000	60 - 120	$2 < y < 4.5$	$p_{T\ell} > 20$ GeV $2 < \eta_\ell < 4.5$	[86]
LHCb 8 TeV	7	$d\sigma/dq_T$	8000	60 - 120	$2 < y < 4.5$	$p_{T\ell} > 20$ GeV $2 < \eta_\ell < 4.5$	[87]
LHCb 13 TeV	7	$d\sigma/dq_T$	13000	60 - 120	$2 < y < 4.5$	$p_{T\ell} > 20$ GeV $2 < \eta_\ell < 4.5$	[92]
CMS 7 TeV	4	$(1/\sigma)d\sigma/dq_T$	7000	60 - 120	$\|y\| < 2.1$	$p_{T\ell} > 20$ GeV $\|\eta_\ell\| < 2.1$	[88]
CMS 8 TeV	4	$(1/\sigma)d\sigma/dq_T$	8000	60 - 120	$\|y\| < 2.1$	$p_{T\ell} > 15$ GeV $\|\eta_\ell\| < 2.1$	[89]
ATLAS 7 TeV	6 6 6	$(1/\sigma)d\sigma/dq_T$	7000	66 - 116	$\|y\| < 1$ $1 < \|y\| < 2$ $2 < \|y\| < 2.4$	$p_{T\ell} > 20$ GeV $\|\eta_\ell\| < 2.4$	[93]
ATLAS 8 TeV on-peak	6 6 6 6 6 6	$(1/\sigma)d\sigma/dq_T$	8000	66 - 116	$\|y\| < 0.4$ $0.4 < \|y\| < 0.8$ $0.8 < \|y\| < 1.2$ $1.2 < \|y\| < 1.6$ $1.6 < \|y\| < 2$ $2 < \|y\| < 2.4$	$p_{T\ell} > 20$ GeV $\|\eta_\ell\| < 2.4$	[90]
ATLAS 8 TeV off-peak	4 8	$(1/\sigma)d\sigma/dq_T$	8000	46 - 66 116 - 150	$\|y\| < 2.4$	$p_{T\ell} > 20$ GeV $\|\eta_\ell\| < 2.4$	[90]
Total	353	-	-	-	-	-	-

[Bacchetta *et al.*, *JHEP* 07 (2020) 117, arXiv:1912.07550]

- Only data with $q_T / Q < 0.2$ (TMD factorisation region).

PV19 fit: Drell-Yan data

$$\left(\frac{d\sigma}{dq_T}\right)_{\text{res.}} \overset{\text{TMD}}{=} \sigma_0 H(Q) \int d^2\mathbf{b}_T e^{i\mathbf{b}_T\cdot\mathbf{q}_T} F_1(x_1, \mathbf{b}_T, Q, Q^2) F_2(x_2, \mathbf{b}_T, Q, Q^2)$$

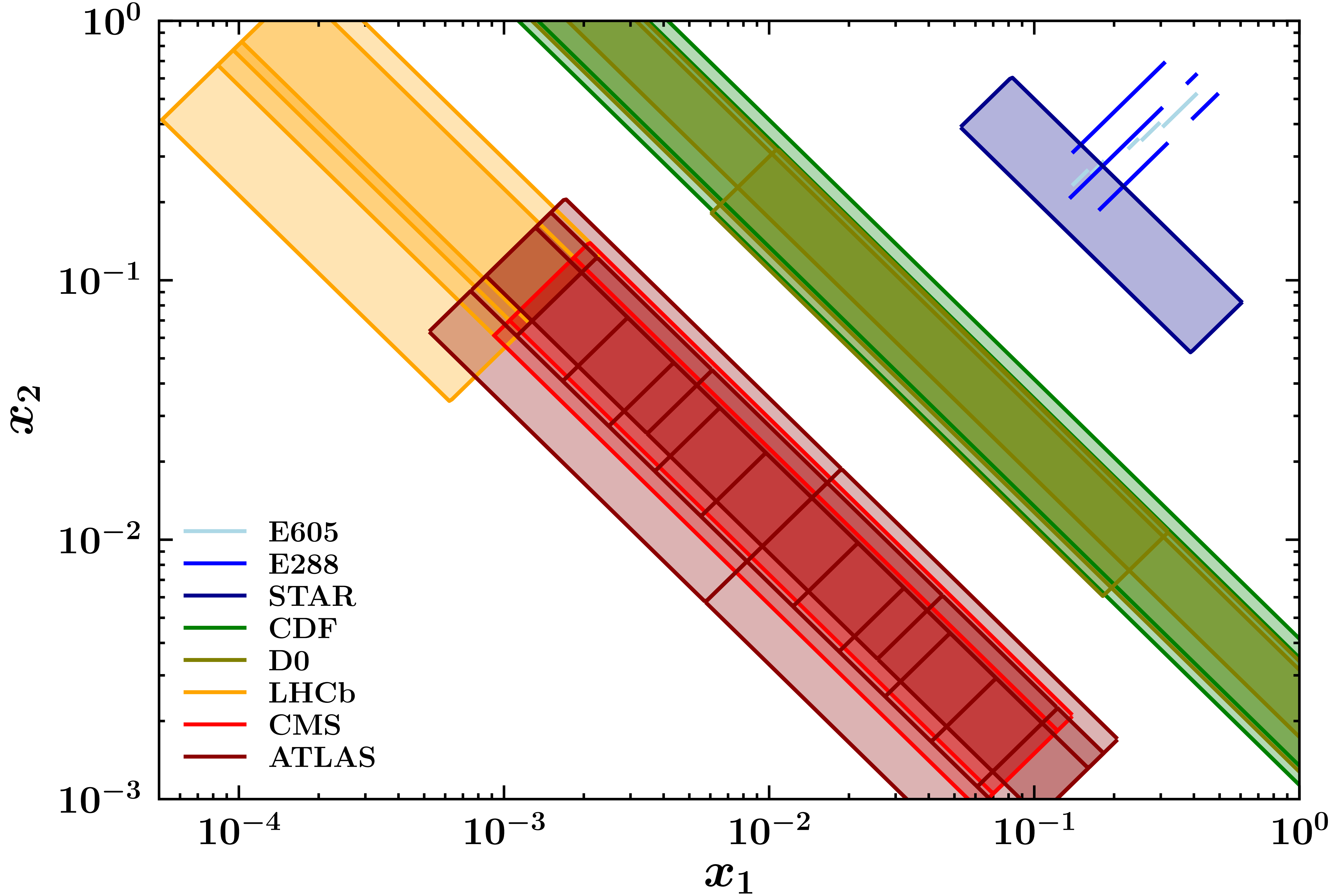

PV19 fit

Fit quality at N^3LL

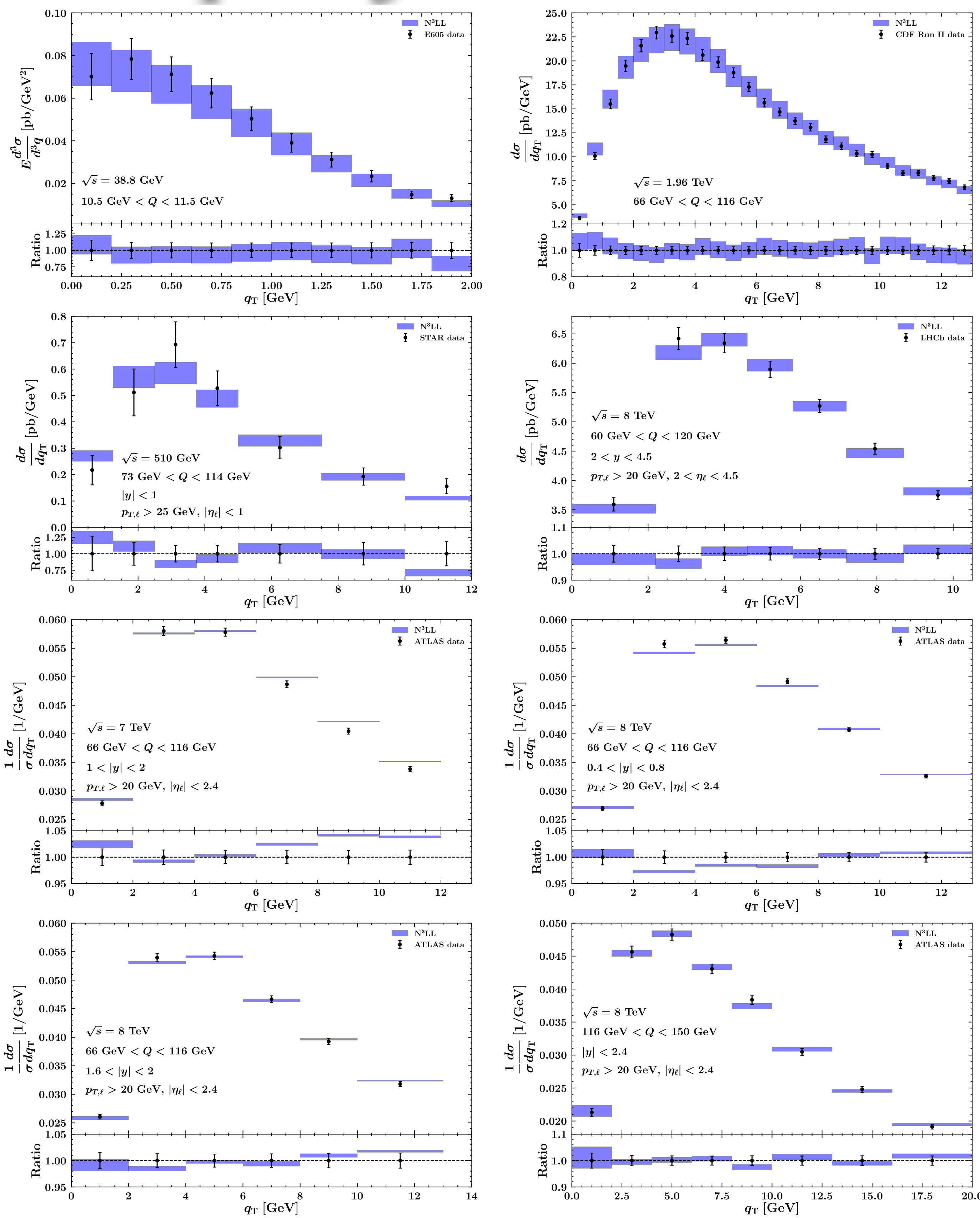

Experiment		χ^2_D/N_{dat}	χ^2_λ/N_{dat}	χ^2/N_{dat}
E605	7 GeV < Q < 8 GeV	0.419	0.068	0.487
	8 GeV < Q < 9 GeV	0.995	0.034	1.029
	10.5 GeV < Q < 11.5 GeV	0.191	0.137	0.328
	11.5 GeV < Q < 13.5 GeV	0.491	0.284	0.775
	13.5 GeV < Q < 18 GeV	0.491	0.385	0.877
E288 200 GeV	4 GeV < Q < 5 GeV	0.213	0.649	0.862
	5 GeV < Q < 6 GeV	0.673	0.292	0.965
	6 GeV < Q < 7 GeV	0.133	0.141	0.275
	7 GeV < Q < 8 GeV	0.254	0.014	0.268
	8 GeV < Q < 9 GeV	0.652	0.024	0.676
E288 300 GeV	4 GeV < Q < 5 GeV	0.231	0.555	0.785
	5 GeV < Q < 6 GeV	0.502	0.204	0.706
	6 GeV < Q < 7 GeV	0.315	0.063	0.378
	7 GeV < Q < 8 GeV	0.056	0.030	0.086
	8 GeV < Q < 9 GeV	0.530	0.017	0.547
	11 GeV < Q < 12 GeV	1.047	0.167	1.215
E288 400 GeV	5 GeV < Q < 6 GeV	0.312	0.065	0.377
	6 GeV < Q < 7 GeV	0.100	0.005	0.105
	7 GeV < Q < 8 GeV	0.018	0.011	0.029
	8 GeV < Q < 9 GeV	0.437	0.039	0.477
	11 GeV < Q < 12 GeV	0.637	0.036	0.673
	12 GeV < Q < 13 GeV	0.788	0.028	0.816
	13 GeV < Q < 14 GeV	1.064	0.044	1.107
STAR		0.782	0.054	0.836
CDF Run I		0.480	0.058	0.538
CDF Run II		0.959	0.001	0.959
D0 Run I		0.711	0.043	0.753
D0 Run II		1.325	0.612	1.937
D0 Run II (μ)		3.196	0.023	3.218
LHCb 7 TeV		1.069	0.194	1.263
LHCb 8 TeV		0.460	0.075	0.535
LHCb 13 TeV		0.735	0.020	0.755
CMS 7 TeV		2.131	0.000	2.131
CMS 8 TeV		1.405	0.007	1.412
ATLAS 7 TeV	0 < |y| < 1	2.581	0.028	2.609
	1 < |y| < 2	4.333	1.032	5.365
	2 < |y| < 2.4	3.561	0.378	3.939
ATLAS 8 TeV on-peak	0 < |y| < 0.4	1.924	0.337	2.262
	0.4 < |y| < 0.8	2.342	0.247	2.590
	0.8 < |y| < 1.2	0.917	0.061	0.978
	1.2 < |y| < 1.6	0.912	0.095	1.006
	1.6 < |y| < 2	0.721	0.092	0.814
	2 < |y| < 2.4	0.932	0.348	1.280
ATLAS 8 TeV off-peak	46 GeV < Q < 66 GeV	2.138	0.745	2.883
	116 GeV < Q < 150 GeV	0.501	0.003	0.504
Global		**0.88**	**0.14**	**1.02**

PV19 fit
Perturbative convergence

- Global χ^2 as a function of the perturbative accuracy:

Order	NLL	NLL'	NNLL	NNLL'	N^{3}LL
χ^2 / n.d.p.	~20	3.19	1.62	1.07	1.02

- Clear perturbative **convergence**.

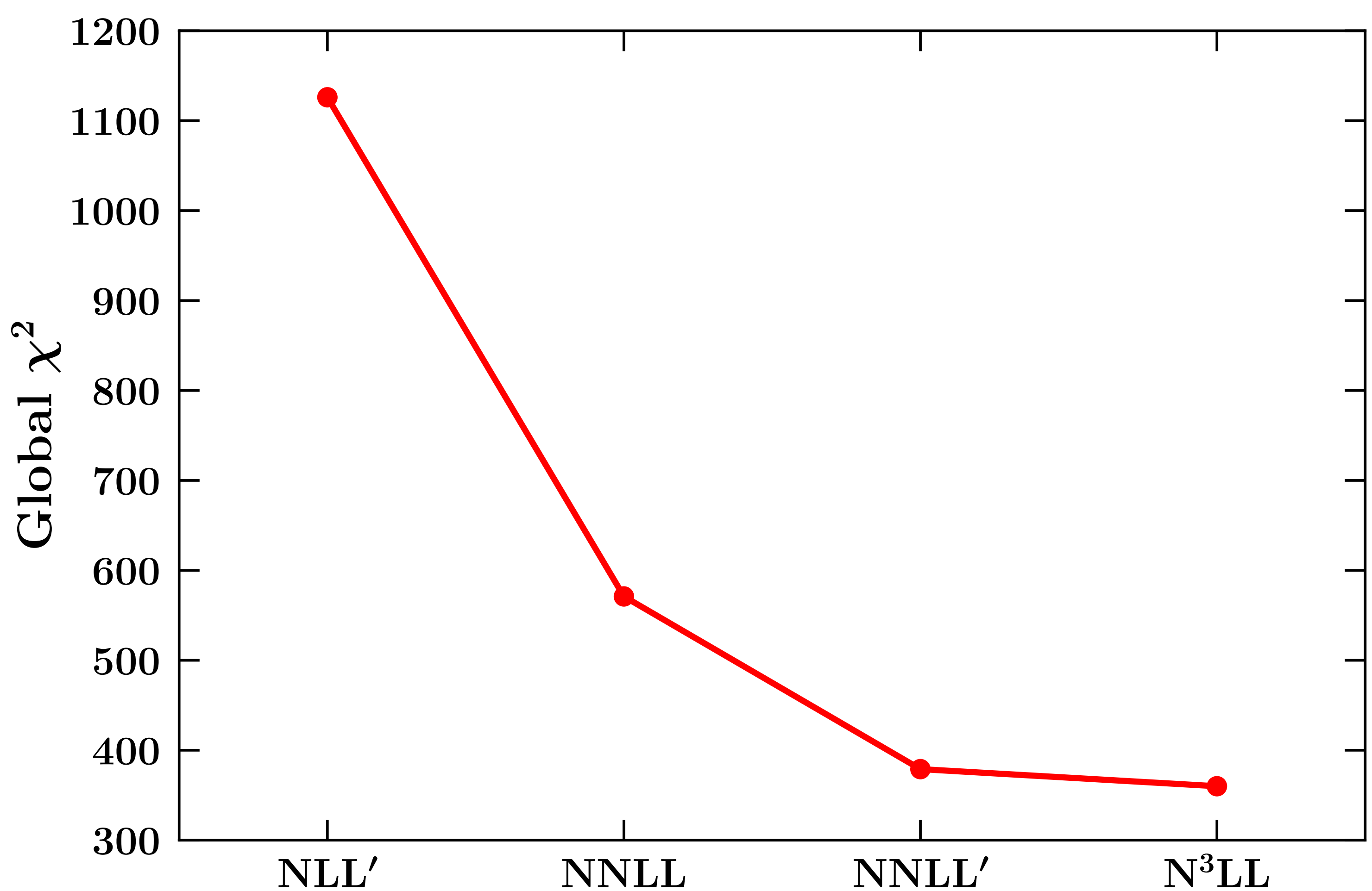

PV19 fit

Perturbative convergence

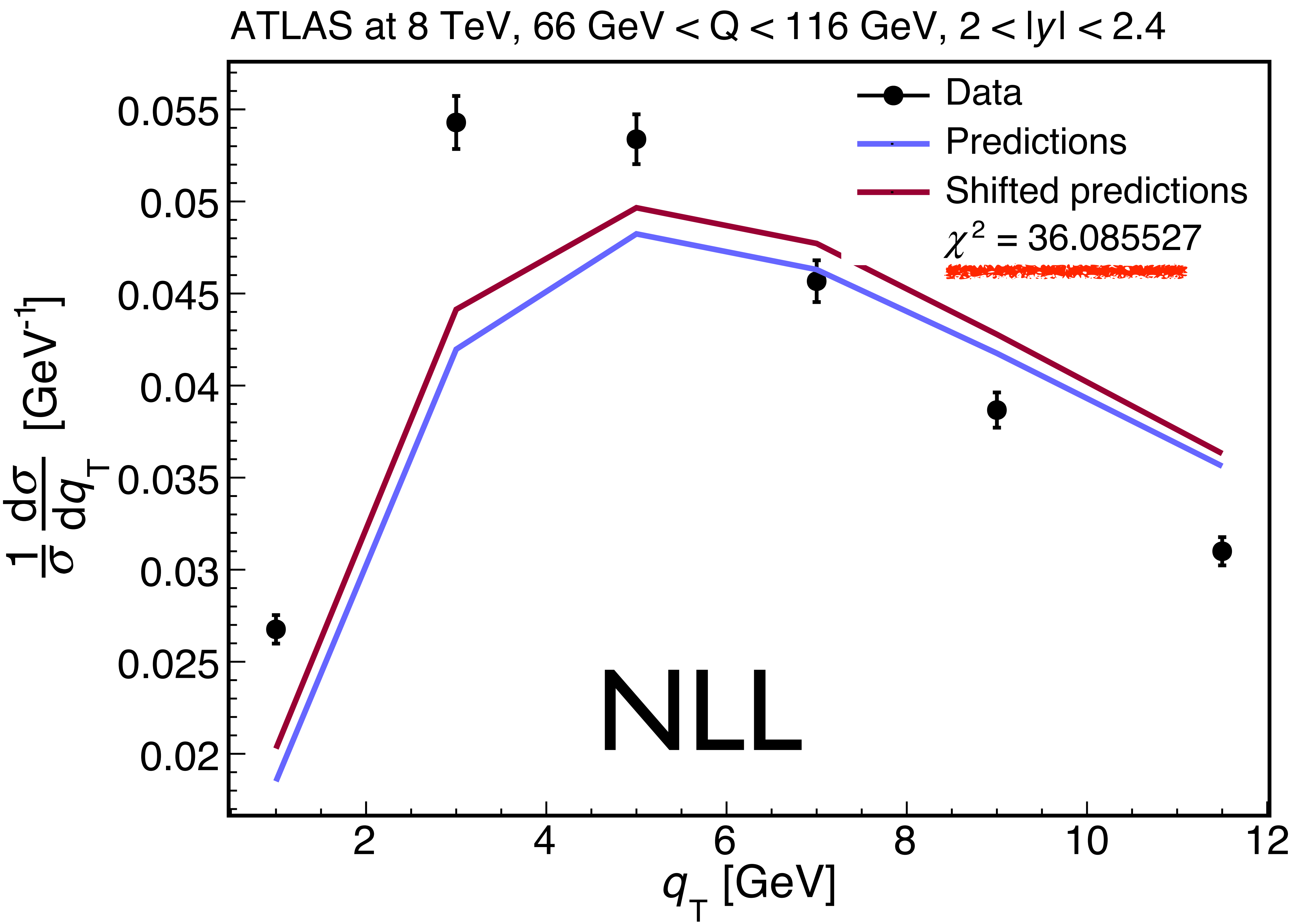

PV19 fit

Perturbative convergence

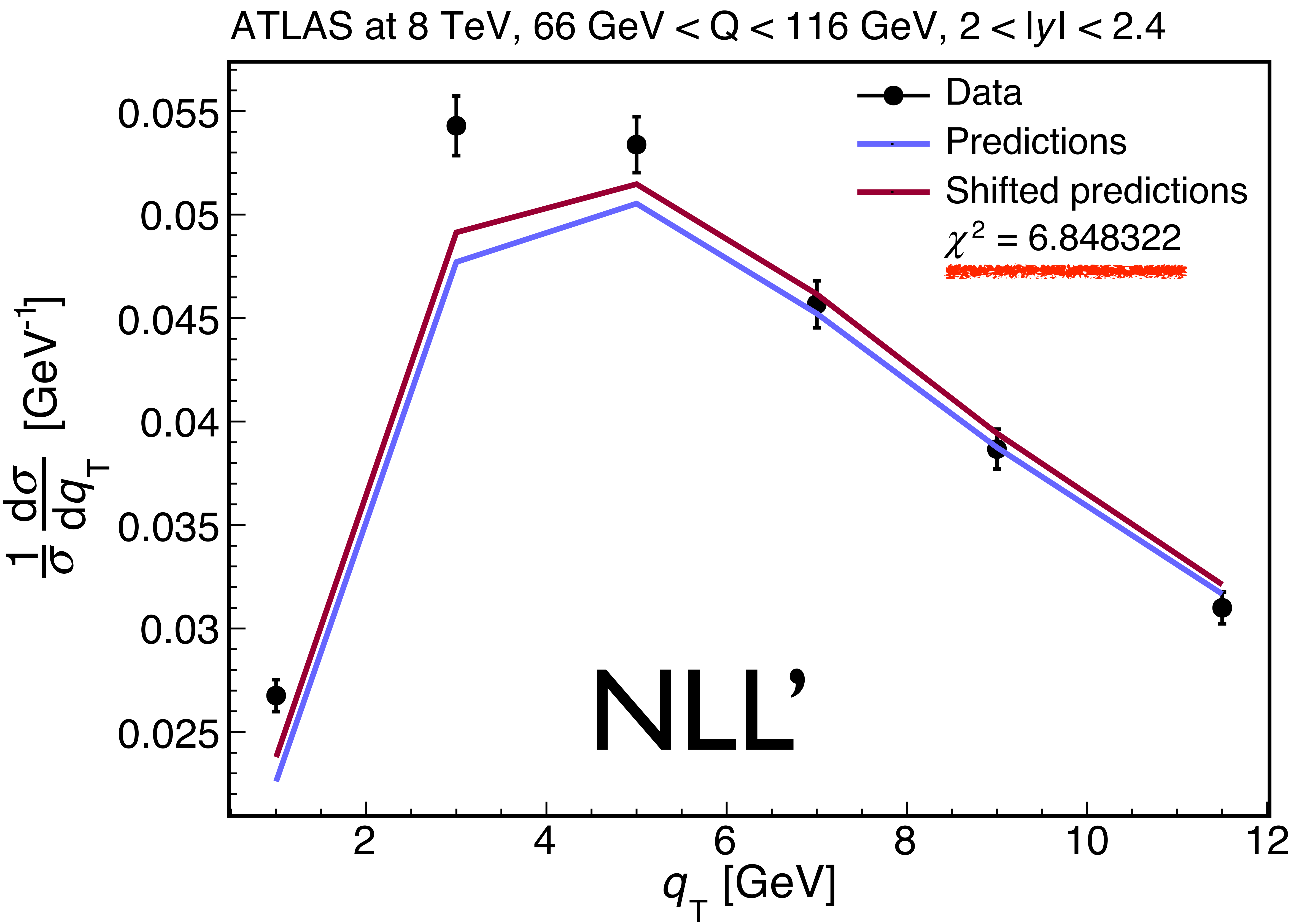

PV19 fit

Perturbative convergence

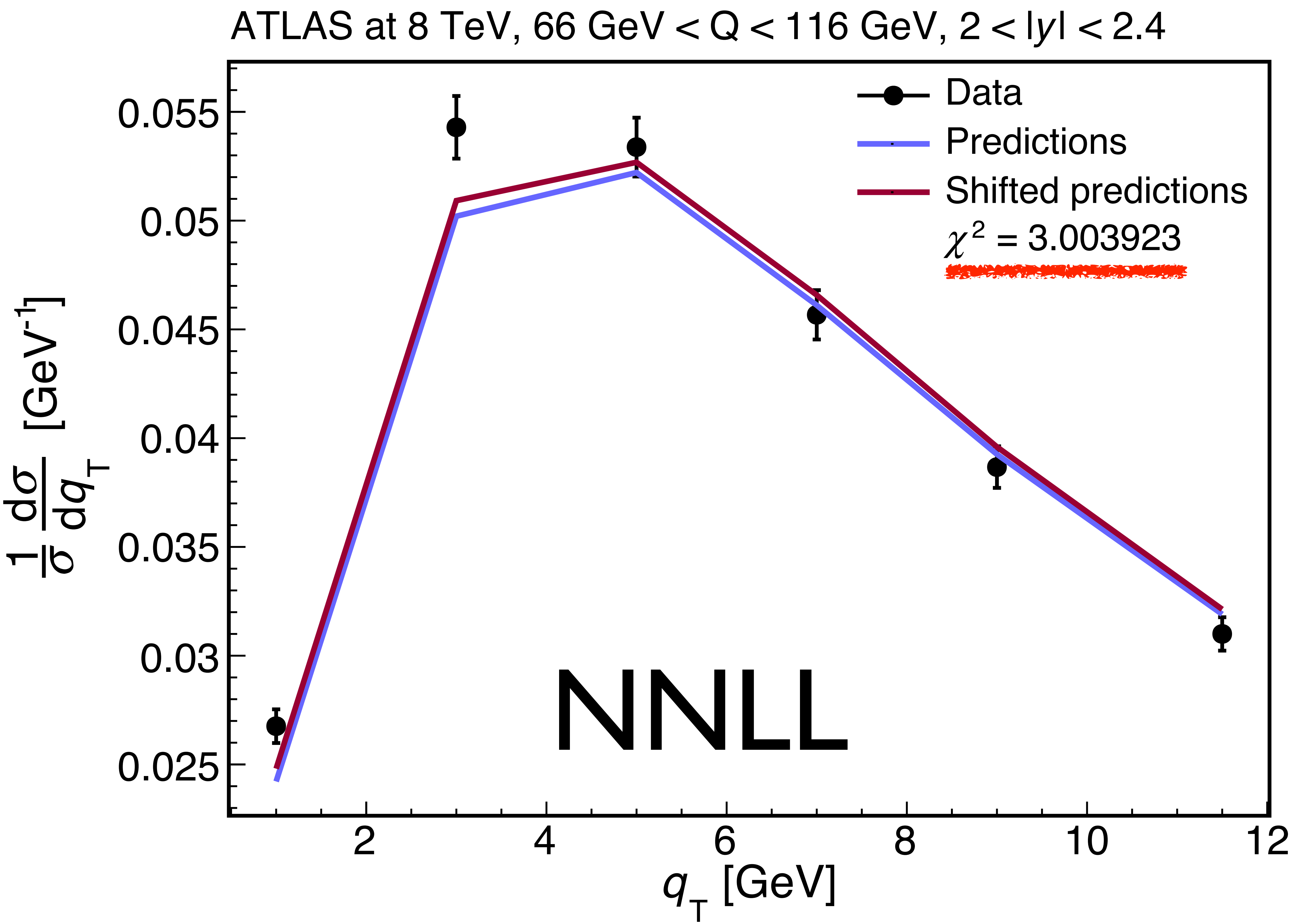

PV19 fit
Perturbative convergence

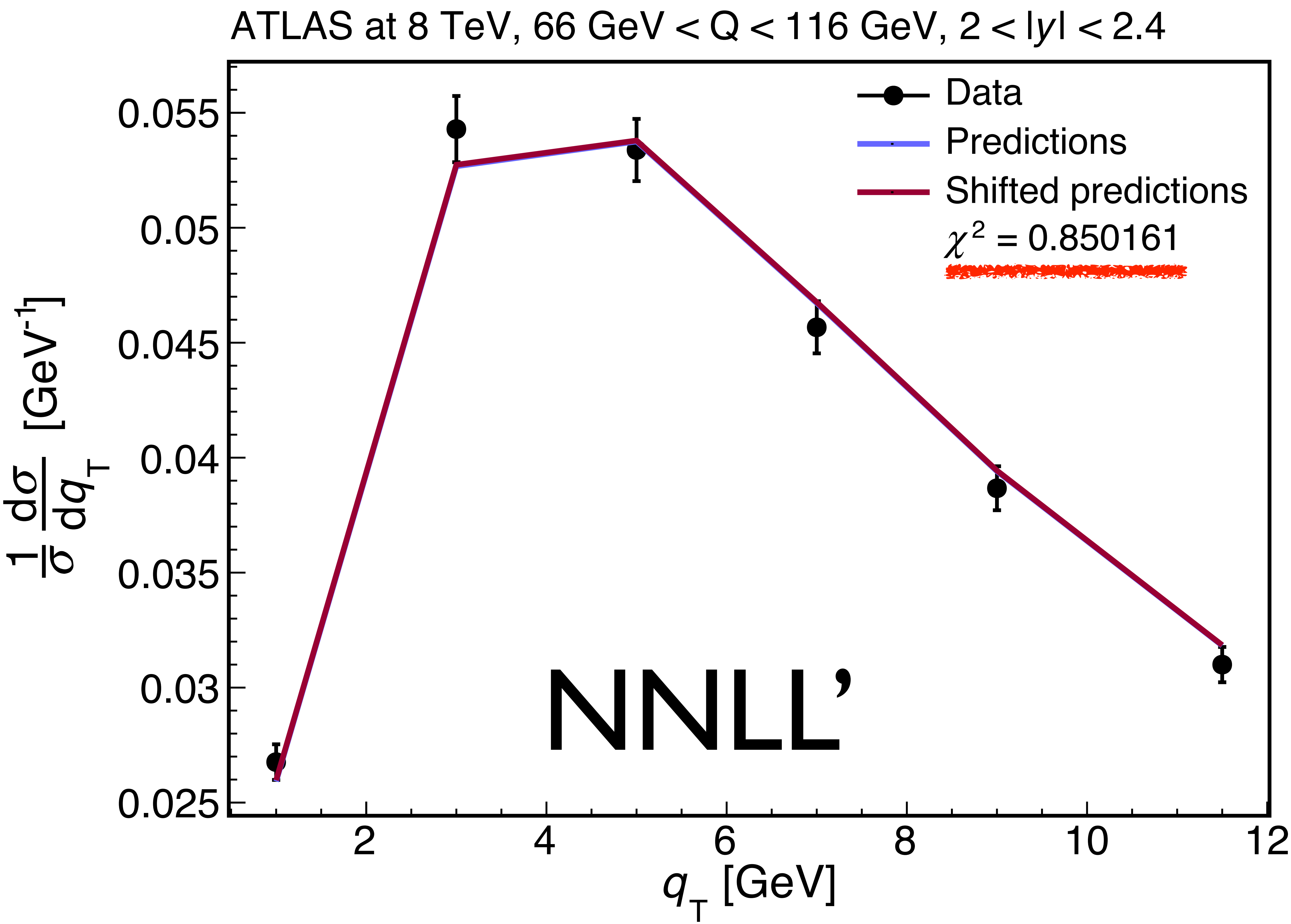

PV19 fit

Perturbative convergence

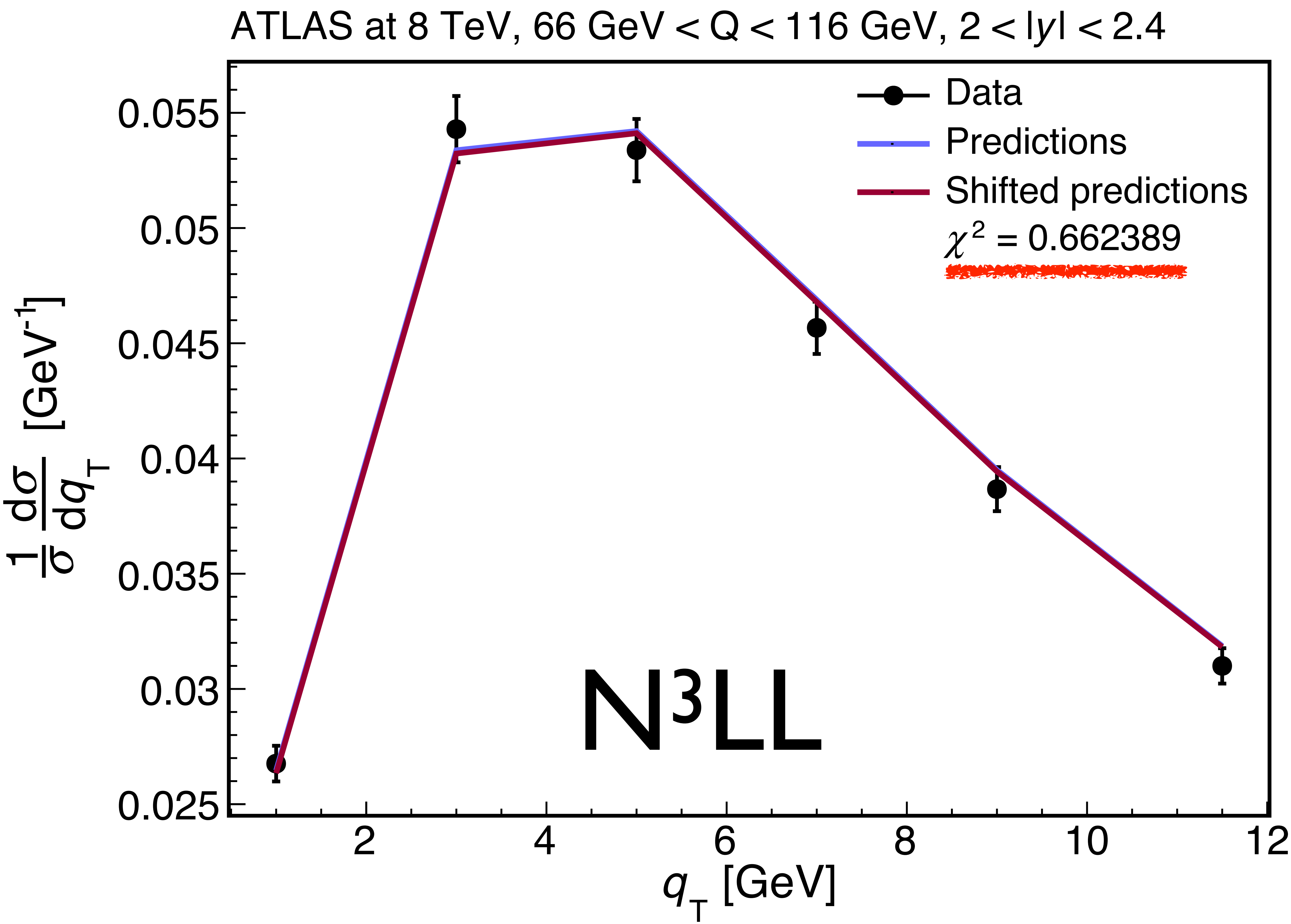

Conclusions and outlook

- A lot of effort is being invested on the extraction of TMD PDFs and FFs:
  - wide and precise **datasets** (LHC and Tevatron exps., COMPASS, HERMES),
  - very accurate **theoretical computation** (N^3LL at small q_T),
- Current precision of data does require the most accurate **calculations**:
  - perturbative convergence.
- A sound treatment of the **experimental** uncertainties is also required:
  - correlated systematics,
  - collinear PDF uncertainties.
- Outstanding issues concerning **SIDIS** data from COMPASS/HERMES.
- Also **e^+e^- annihilation** data will be considered to constrain TMD FFs.
- **Current experiments** have still much to say on TMDs.
- Looking forward to the **EI(c)C** for more data to constrain TMDs.